

Microwave ionization of Rydberg states of the barium ion

M. Seng¹, U. Eichmann^{1,a}, V. Lange², T.F. Gallagher³, and W. Sandner^{1,4}

¹ Max-Born-Institut for Nonlinear Optics and Short Pulse Spectroscopy, 12489 Berlin, Germany

² Fachhochschule Furtwangen, 78120 Furtwangen, Germany

³ University of Virginia, Charlottesville, VA 22901, USA

⁴ Technical University Berlin, 10268 Berlin, Germany

Received: 17 September 1996 / Revised: 6 April 1998 / Accepted: 8 April 1998

Abstract. We have investigated the electric field ionization of highly excited (ns) and (nd) Rydberg states of the barium ion by microwave fields. For states with a principal quantum number $n \leq 40$ the observed microwave ionization threshold fields show the $Z^3/3n^5$ dependence expected on the basis of previously observed ionization of neutral Rydberg states with $Z = 1$. We show that for states in this n regime microwave ionization is a state selective detection technique. Threshold fields for states with $n > 40$, however, depart from the expected behaviour, the thresholds become broader and shift to higher fields. For a total of 58 states we present the field strengths where 90%, 50% and 10% ionization occur.

PACS. 31.50.+w Excited states – 32.30.Jc Visible and ultraviolet spectra – 32.80.Rm Multiphoton ionization and excitation to highly excited states (e.g., Rydberg states)

1 Introduction

In the last decade various experiments have been reported on the interaction of highly excited helium, alkali, and alkaline earth atoms with strong microwave fields [1–6]. One surprising common aspect of these experiments was the observation of a new simple scaling law for ionization in a linearly polarized microwave field. In the low frequency regime, in which the microwave frequency is much less than the n spacing the threshold fields for microwave ionization of states with low m , where m is the azimuthal angular momentum quantum number, follow a $1/3n^5$ scaling law (in a.u.), where n is the principal quantum number of the Rydberg state. These fields are considerably lower than the corresponding static field ionization thresholds which scale as $1/16n^4$, following the classical saddle point ionization model [7].

They are also much lower than the microwave ionization fields for hydrogen and hydrogen like higher m states of alkali atoms. For these states, in the low frequency regime the ionization fields are given by $E = 1/9n^4$, which is the field at which the lowest $m = 0$ Stark state ionizes in a static field [1, 8].

A straightforward explanation for the unexpected new scaling law for microwave ionization with linear microwave fields was presented by Pillet *et al.* [9], who gave a single cycle Landau Zener picture. At a field strength of $1/3n^5$ the highest energy $m = 0$ member of the Stark manifold of principal quantum number n intersects the lowest energy $m = 0$ member of the adjacent Stark manifold with

principal quantum number $n + 1$. At this point, there is an avoided crossing between the two levels, and a Landau Zener transition from n to $n + 1$ can occur, which is thus the rate limiting step in the process of microwave ionization, which proceeds then by a sequence of $n \rightarrow n + 1$ transitions culminating in ionization.

In experiments subsequent to the initial ionization experiments microwave multiphoton transitions analogous to the rate limiting $n \rightarrow n + 1$ transitions of ionization were observed between bound Rydberg states [10–12]. These experiments and the accompanying analyses showed that when the single cycle Landau–Zener description was extended to more than one cycle the interference between the transition amplitudes from different field cycles developed into multiphoton resonances. These experiments also showed that, due to the constructive interference at resonance to the $n \rightarrow n + 1$ transitions could be driven by microwave fields as much as 30% lower than $F = 1/3n^5$, in agreement with the experimental finding [1].

Experiments both on static and microwave field ionization have been almost entirely restricted to neutral Rydberg states. One expects ionic Rydberg states to differ from neutral Rydberg states only by their different core charge, *i.e.* $Z = 2$ instead of $Z = 1$. Explicitly, we would expect the classical static field ionization field to be given by $E = Z^3/16n^4$ and the microwave ionization field of low m non hydrogenic ions to be given by $E = Z^3/3n^5$. The Z^3 factor originates from a Z^2 due to the binding energy and a Z due to the size of the atom. For a singly charged ion the ionization fields are eight times as large as those for a neutral atom of the same n . Static field

^a e-mail: eichmann@mbi-berlin.de

ionization has proved to be an invaluable tool for state selective detection of neutral Rydberg atoms. It has been used to detect microwave transitions, the final states of collisions, and the population redistribution due to laser pulses [13–15]. Static field ionization has already been shown to be an important tool to detect ionic Rydberg states either produced by laser excitation [16] or stemming from the decay of doubly excited states [17–19]. Ionic states as low as $n = 25$ have been detected. Microwave ionization has two major advantages when compared to static field ionization. First, a microwave field strength of the same magnitude as a static field can ionize Rydberg states with much lower principal quantum number. Second, since the microwave field is rapidly oscillating, the ionic Rydberg states are not driven out of the interaction region before they are completely ionized. Therefore, very high field strengths can be used to ionize the Rydberg ions before they are expelled from the ionization volume.

We thus investigated the microwave ionization of ionic Rydberg states in barium and quantitatively determined the threshold behaviour of such states. Boulmer *et al.* have already used a microwave ionization technique to obtain spectroscopic results on barium Rydberg states [20]. However, they did not report any threshold scaling laws, and therefore did not determine how *selective* the microwave ionization technique can be. Our results reported in the present work provide an answer to this question.

2 Experimental apparatus

The essential idea of our experiment is quite simple. Using two pulsed dye lasers we ionize Ba atoms in an atomic beam and excite them to Ba^+ns and nd Rydberg states. The excitation takes place at the center of a Fabry-Perot microwave cavity, and a pulse of microwaves is used to ionize the Ba^+ Rydberg ions. The resulting Ba^{++} ions are swept from the cavity with 100 V/cm field pulse and separated from Ba^+ ions by their time of flight to the detector.

Figure 1 illustrates the excitation scheme we used in our experiment. An excimer laser pumped dye laser with 15 mJ pulse energy at a wavelength of 531.3 nm photoionizes with three photons the barium ground state atoms, leaving a substantial fraction of the barium ions in the metastable $Ba^+5d_{3/2}$ state. Three more photons of the same dye laser resonantly excite the $Ba^+5d_{3/2}$ ions to the $Ba^+8p_{1/2}$ state. Using a second dye laser of about 2 mJ pulse energy, pumped by the same excimer laser, enables us to excite Ba^+ns and Ba^+nd Rydberg states with one additional laser photon. The pulse energies of the two lasers are chosen so that the Rydberg excitation efficiently competes with the direct photoionization of the $Ba^+8p_{1/2}$ state by two more photons of the first laser. The maximum Ba^{2+} ion yield stemming from a Rydberg state accounts for 40 to 80% of the total Ba^{2+} yield, depending which n state is excited. By scanning the wavelength of the second laser with the maximum available microwave field strength, we obtain a Rydberg spectrum of Ba^+ns

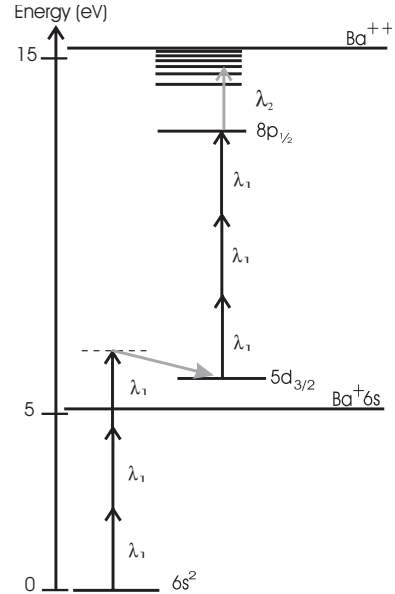


Fig. 1. Excitation scheme used to excite ionic barium Rydberg states. A strong ($\sim 10^9$ W/cm²) laser excites with resonantly enhanced two three photon transitions at a fixed wavelength of 531.1 nm neutral Ba ground state atoms to the $Ba^+(8p_{1/2})$ state ~ 2.4 eV below the Ba^{2+} threshold. A second dye laser then drives the transition into the Rydberg region. For details see text.

and nd states. The wavelength is calibrated simultaneously recording the Fabry-Perot fringes of a solid etalon as well as an optogalvanic spectrum of an Argon lamp, and the spectrum allows unambiguous assignment of the Ba^+ states.

To measure microwave ionization threshold fields we excite individual Rydberg states and record the Ba^{2+} yield as a function of the microwave field strength. The simultaneously recorded Ba^+ yield can be used for normalization to account for oven fluctuations as well as intensity fluctuations of the strong dye laser that drives the two three photon transitions.

An HP 8473B crystal detector is attached to one side of the cavity volume. This detector is used to monitor the power in the cavity, allowing us to tune the mirror distance in 10 μ m steps to keep the cavity in resonance with the magnetron. After a warm-up time of approximately 10 minutes the magnetron frequency is stable and further tuning of the resonator was found to be unnecessary.

The basic experimental setup consists of a crossed atomic-laser-beam arrangement and has already been described in detail elsewhere [17]. The new component in our setup is a Fabry Perot microwave cavity, located around the laser-atom interaction center. It consists of two spherical brass mirrors facing each other, separated by a distance of about 9 cm. The mirror axis coincides with the laser beam axis. The laser beams are focused with a 30 cm focal length lens before entering the vacuum chamber and then enter and exit the cavity through 2 mm diameter holes in the resonator mirrors, being focused at the center of the cavity. An effusive beam of barium atoms

also passes through the center of the cavity between two field plates where it is intersected by the laser beams at an angle of 90° . The field plates are separated from each other by 10 cm, so that they do not affect the standing microwave field in the center of the cavity. The field plates each have a 3 mm diameter hole. One hole enables the barium ions to be extracted out of the interaction region by applying a small electric field pulse. The ions are then detected in a dual microchannel-plate time of flight detector with a total path length of 15 cm, allowing us to charge discriminate between singly and doubly charged ions. 100 ns after the ionic Rydberg states are excited a 600 ns long microwave pulse is applied, ionizing the Rydberg ions. 200 ns after the microwave pulse a $1 \mu\text{s}$ long static field pulse of 100 V/cm field strength accelerates the doubly charged ions, as well as singly charged ions, – which are inevitably present – towards the detector. The time resolved Ba^+ and Ba^{++} signals from the detector are then recorded with gated integrators. With the above mentioned value of the field strength of the static field pulse no ionic Rydberg state with a principal quantum number n lower than 71 can be field ionized.

Our microwave source is a Furuno FR-1201 magnetron, which produces microwave pulses of 5 kW power and 600 ns duration, at a frequency of 9403 MHz. The power output of the microwave oscillator, shown in Figure 2a is quite reproducible from shot to shot, and matches the specified pulse length of 600 ns. The specified bandwidth of the oscillator is 2.5 MHz, slightly above the Fourier transform limit of 1.7 MHz. To characterize the bandwidth more accurately, we have mixed the output of the magnetron with a cw oscillator at 9415.5 MHz and observed the beat signal, as shown in Figure 2b. Measuring the periods of the beat signal shows that the instantaneous frequency of the magnetron varies as shown in Figure 2c, *i.e.* the frequency oscillates by about 2.5 MHz during the pulse but does not exhibit an obvious chirp. A Fourier transform of the beat signal of Figure 2b also shows a width of 2 MHz, consistent with the analysis of the periods. The output of the magnetron can, in principle, be fed directly into our Fabry Perot cavity, producing a maximum field strength of roughly 10 kV/cm in the cavity. For the measurements the microwave power is passed through a 14 dB fixed X-band attenuator to reduce the pulse power to 200 W and then through a high precision Weinschel AE 9003 step attenuator (0 to 69 dB, calibrated), which can be used to control the power in 1 dB steps ($\pm 1\%$ uncertainty for each step). All cable connections are designed to be as short as possible with 0.141 inch semirigid cable and SMA connectors.

The Fabry Perot cavity is designed to operate in the TEM_{004} fundamental mode, having an antinode in its center where excitation and ionization of the barium atoms and ions occurs. The radius of curvature of both mirrors is 17 cm and both have a diameter of 11.6 cm.

The microwave power is brought into the vacuum chamber *via* a semi rigid coaxial cable to a waveguide to coaxial adapter attached to the back of one of the cavity mirrors. The microwaves are coupled into the cavity

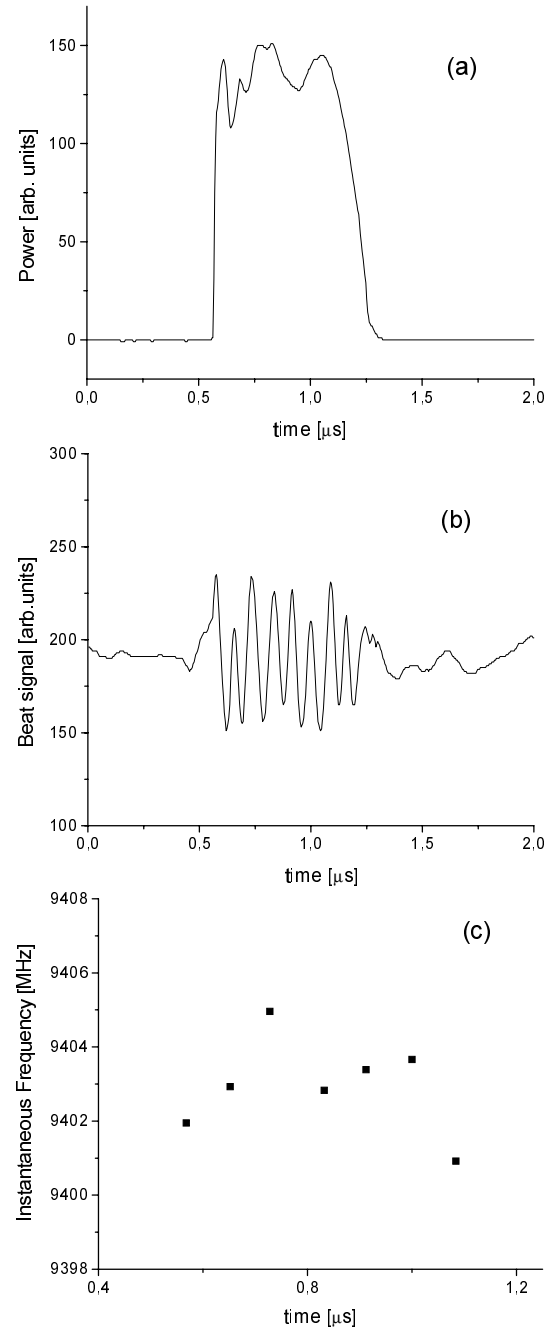


Fig. 2. (a) Power output of the magnetron pulse at 9403 MHz. (b) Observed beat signal obtained when mixing the magnetron output with the 9415.5 MHz output of the continuous wave oscillator. (c) Instantaneous frequency of the magnetron during the pulse. It is obtained by measuring periods of successive cycles of beat signals such as the one shown in (b).

through an 8 mm diameter iris, and the linear polarization of the microwave field in the cavity is parallel to the short wall of the waveguide. With this arrangement measurement of the frequency dependence of the reflected power gives a Q of 5000 ± 200 and a $93 \pm 5\%$ efficiency for coupling power into the cavity.

The backside of the waveguide to coaxial adapter also has a 2 mm diameter hole in its center, allowing the laser pulses to travel through the waveguide piece into the cavity along its symmetry axis and exit through a 2 mm diameter hole in the opposite mirror. Although we can measure the cavity parameters and the pulse shape and frequency dependence of the magnetron, we are unable to measure its power in a complete satisfactory way. Therefore we have chosen to calibrate the microwave field using the known field strength values for microwave ionization of Ba $6snd$ Rydberg states [4]. The Ba $6s23d$ and the $6s25d$ states were chosen as “calibration points”.

Excitation of these states is performed by a resonant two laser process. A second excimer laser is used to pump these two additional dye lasers. One dye laser excites barium ground state atoms to the intermediate $6s6p$ state and the second laser drives the transition to the Rydberg states. Then we measure the Ba^{++} yield as a function of the setting of our step attenuator. The field strengths for the 50% ionization rates of these states are measured to be $364 \text{ V/cm} \pm 10\%$ for the Ba $6s23d$ state and $244 \text{ V/cm} \pm 10\%$ for the Ba $6s25d$ state [4]. Thus, the setting of the step attenuator at which 50% ionization of one of these states occurs is directly connected with these field strength values in the Fabry Perot resonator. Both “calibration points” independently lead to a 0 dB value (which equals maximum power transmission) of $1490 \text{ V/cm} \pm 12\%$. These measurements were frequently repeated during the microwave ionization experiment of barium ion Rydberg states, to ensure the stability of the calibration. The overall error of $\pm 12\%$, that we assign to our values, is calculated from the error given by Eichmann *et al.* [4] ($\pm 10\%$), and the error stemming from our calibration measurements ($\pm 7\%$).

3 Results and discussion

With a maximum field strength of 1490 V/cm in the microwave cavity, we should be able to completely ionize Ba^{++} Rydberg states with principal quantum number n as low as 25, assuming that the expected $\frac{Z^3}{3n^5}$ scaling law is valid.

Unlike many properties of non hydrogenic atoms, the microwave ionization fields do not depend on the precise quantum defects, rather on the n value of the nearest hydrogenic levels. Therefore the $Ba^{++}ns$ states, which have quantum defects of 3.58, are nearest to the $n - 4$ hydrogenic levels and are assigned n values four lower than their nominal values. The nd states, with quantum defects of 2.38, are nearest to the hydrogenic $n - 2$ states and are assigned n values two lower than their nominal values. For example, the $Ba^{++}29s$ and $27d$ states are both assigned the value $n = 25$. From this point on, an n value without an ℓ always refers to the n value defined above.

For a total of 58 ionic Rydberg states, we measured the Ba^{2+} yield as a function of the microwave field and states with n up to 65 have been included. This upper boundary is determined by the bandwidth of the second dye laser

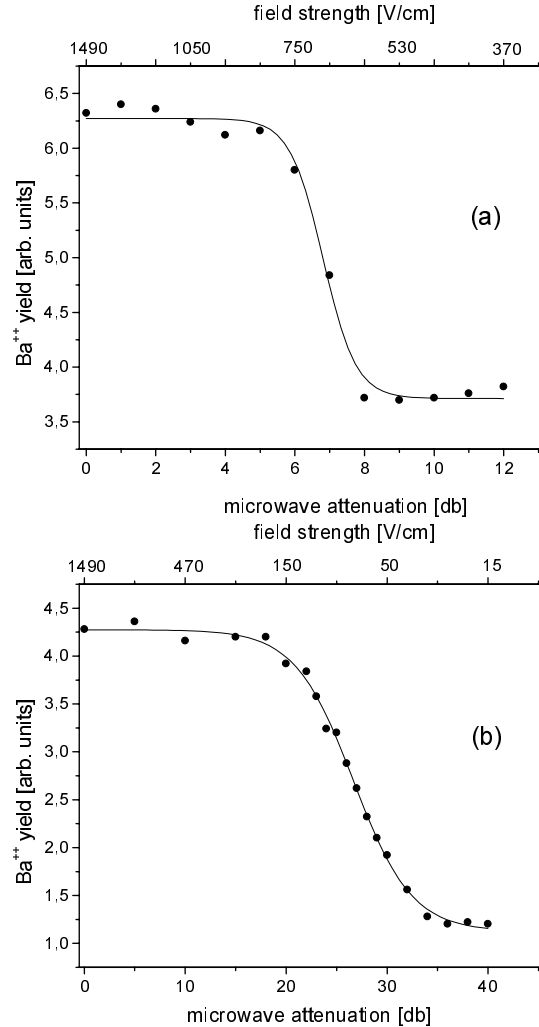


Fig. 3. (a) Measured Ba^{++} yield (circles) stemming from microwave ionization of the $Ba^{++}30d$ Rydberg state as a function of the microwave attenuation (dB). The upper x axis shows the corresponding field strength values. The threshold at 680 V/cm is clearly visible. The straight line is a fit with a phenomenological function. For details see text. (b) Same as in (a), but for the $Ba^{++}53d$ state.

of $\sim 0.3 \text{ cm}^{-1}$, which limits the resolution of s and d states. We measure the microwave ionization thresholds by monitoring the Ba^{++} signal as the microwave power is varied in 1 dB steps. Typical data are shown in Figure 3.

Figure 3a shows the threshold behaviour observed after excitation of the $Ba^{++}30d$ state and Figure 3b corresponds to the $Ba^{++}53d$ state. The spectrum of the $Ba^{++}30d$ state shows a rather sharp threshold, whereas the $Ba^{++}(53d)$ state threshold is very broad. In general we observe, within our microwave resolution of 1 dB, for all states a smooth and monotonic decline of the ionization yield as the microwave field strength is decreased. Resonance structures in the ionization are not observed for any ionic Rydberg state.

Inspection of the data shows that with increasing n the observed thresholds become broader. We decided to

Table 1. Ionization fields of the Ba^+ (ns) states.

$\text{Ba}^+(ns)$	n	p_3	$F_{90\%}$ (V/cm)	$F_{50\%}$ (V/cm)	$F_{10\%}$ (V/cm)
29	25	1.04	1503	1331	1205
30	26	0.83	1192	1024	879
31	27	0.80	878	749	640
32	28	0.88	880	761	659
33	29	0.79	726	618	526
34	30	0.95	629	551	482
35	31	0.64	554	455	374
36	32	0.73	458	385	324
37	33	0.91	379	329	287
38	34	0.63	338	277	227
40	36	0.46	303	231	176
42	38	0.68	211	175	145
44	40	0.45	205	155	117
46	42	0.33	191	130	88
48	44	0.36	174	122	86
50	46	0.22	151	84	48
52	48	0.30	122	79	52
54	50	0.21	130	70	38
56	52	0.12	228	79	28
58	54	0.20	110	59	31
61	57	0.14	119	49	20
64	60	0.34	42	29	20
65	61	0.14	96	39	26
66	62	0.16	68	31	20
67	63	0.08	221	46	10
68	64	0.10	148	39	15
69	65	0.11	111	34	15
70	66	0.16	87	39	25
71	67	0.06	283	34	17

describe our data by fitting a phenomenological threshold function to each set. With such a fit, we can obtain threshold values for 90%, 50% and 10% ionization. The symmetric function has the form:

$$S_{(\text{arb. units})} = p_1 + p_2(1 + \tanh(p_3(x_{\text{dB}} - p_4))) \quad (1)$$

S is the signal, which is only known in arbitrary units, x is the microwave attenuation in dB. The parameter p_1 stands for a constant offset, namely the constant photoionization yield stemming from the first laser, $2p_2$ is the maximum microwave ionization yield. p_4 is the microwave attenuation value where 50% ionization is reached, p_3 is a measure of the slope of the function at this point. We note that we also evaluated the calibration thresholds of the neutral barium states with this function and they show a very sharp threshold behaviour.

Tables 1 and 2 summarize our results for all states under investigation. The question of whether or not the Landau Zener ionization picture is valid can best be answered by plotting the ionization threshold values as a

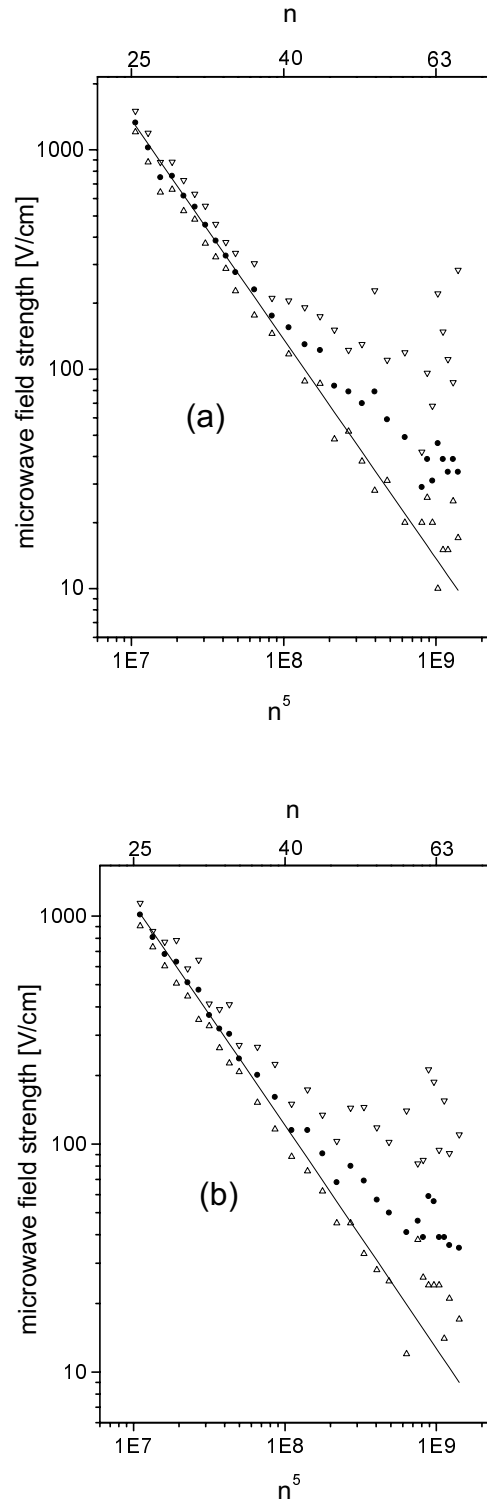


Fig. 4. (a) Double logarithmic plot of the experimentally obtained threshold values at which 90% (open downward triangles), 50% (full circles) and 10% (open upward triangles) ionization for Ba^+nd Rydberg states occur, as a function of n (recall that n is the value of the hydrogenic level nearest to the Ba^+nd state). The straight line represents the expected $Z^3/3n^5$ threshold field. (b) same as in (a) for the Ba^+ns states. Again the straight line follows the $Z^3/3n^5$ dependence.

Table 2. Ionization fields of the Ba⁺ (*nd*) states.

Ba ⁺ (<i>nd</i>)	<i>n</i>	<i>p</i> ₃	<i>F</i> _{90%} (V/cm)	<i>F</i> _{50%} (V/cm)	<i>F</i> _{10%} (V/cm)
28	26	1.08	1141	1016	904
29	27	1.24	895	809	731
30	28	1.04	769	681	603
31	29	0.60	783	630	507
32	30	0.91	588	511	445
33	31	0.42	641	475	351
34	32	1.12	412	368	329
35	33	0.65	390	321	264
36	34	0.43	409	304	226
37	35	0.94	271	237	207
39	37	0.45	266	201	152
41	39	0.38	224	161	116
43	41	0.48	150	115	88
45	43	0.31	173	115	76
47	45	0.33	134	91	62
49	47	0.30	103	68	45
51	49	0.22	144	80	45
53	51	0.17	145	69	33
55	53	0.17	118	57	28
57	55	0.18	102	50	25
60	58	0.11	140	41	12
62	60	0.22	82	46	28
63	61	0.16	85	39	26
64	62	0.10	212	59	24
65	63	0.11	187	56	24
66	64	0.14	94	39	24
67	65	0.09	155	39	14
68	66	0.14	91	36	21
70	68	0.11	110	35	17

function of *n*. Figures 4a and b show these plots for the *s* and *d* states. The double logarithmic plot contains for each state the 90%, 50% and 10% ionization threshold values. The straight lines in Figures 4a and b shows the expected $\frac{Z^3}{3n^5}$ behaviour. Inspecting Figure 4 more carefully, two different regimes of ionization behaviour can be easily distinguished. For *n* < 40, the thresholds are rather sharp, and the 50% ionization field strength values follow the threshold law very closely.

For higher *n*, the thresholds become much broader and the 90% ionization field strength values scatter around the *n* = 40 value of ~ 150 V/cm. The 10% values on the other hand still roughly follow the threshold law.

This deviation for higher principal quantum numbers has also been observed for neutral Rydberg states in sodium [21,22]. A likely explanation of the broadening of the thresholds with increasing *n* is as follows. At low *n* the sequence of *n* → *n* + 1 transitions leading to ionization can be made in a time short to the duration of the microwave pulse length, and the resulting ionization thresholds are

sharp, at $F = \frac{Z^3}{3n^5}$. As *n* is raised the *n* → *n* + 1 avoided crossings decrease, as *n*⁻⁴, resulting in a decrease in the rate at which the *n* → *n* + 1 transitions occur. As a result, with a fixed length of the microwave pulse, while the onset of ionization can still occur at $F = \frac{Z^3}{3n^5}$, complete ionization is likely to require a higher field. Recent experiments showing broadening of the thresholds with decreasing microwave pulse length support this explanation [23].

Inspecting the ionization threshold field strengths for the *s* or *d* states shows that, for *n* < 40, a well defined detection cutoff in *n* can be achieved by setting the field strength to a value slightly below the 50% ionization field strength. For example it is possible to field ionize 50% of the 34*d* states with less than 10% ionization of the 33*d* state and virtually no ionization of lower lying *d* states.

Selective detection of adjacent angular momentum states, in our setup the *s* and *d* states (*e.g.* the 32*d* and the 33*s* state) is also possible, since the field strength value to ionize 50% of the 32*d* state, 511 V/cm, is only sufficient to ionize less than 10% of the 33*s* state (526 V/cm for 10% ionization). We have to note, however, that this angular momentum selectivity is of course limited to certain classes of angular momentum eigenstates, where the limitation depends on the specific Stark structure of the element in question, namely the quantum defects of the different series of Rydberg states. As is known from earlier work on the microwave ionization of sodium atoms [1], states with higher *m* quantum numbers (*|m|* ≥ 2), which can be selectively excited by choosing the appropriate combination of laser polarisations, require a substantially higher microwave field, close to the static field threshold to ionize. In heavier barium atoms, however, such an effect could not be observed [4]. In general it is expected that states with higher angular momentum require higher microwave ionization fields to completely ionize [3].

Finally we mention, that with a field strength of 10 kV/cm ionic states with *n* as low as 17 can be ionized. The microwave apparatus described here can therefore be an important tool in detecting fragmentation products of doubly excited states, especially asymmetrically excited planetary states (*n*₁*l*₁*n*₂*l*₂) where both principal quantum numbers are higher than 17. These states are expected to autoionize preferentially into nearby ionic continua [17–19,24].

4 Conclusion

In summary, we were able to obtain threshold spectra of the microwave ionization of Rydberg states of the barium ion for 58 different states of the *s* and *d* series. For states with an effective quantum number *ν* below 40, we could confirm the Z^3 dependence of the microwave ionization scaling law for a linearly polarized microwave field. States with higher effective quantum numbers show a more and more incomplete ionization rate at the field strength values derived from this scaling law. Moreover, they show

a broadening in their individual threshold spectra, as already observed for neutral Rydberg states, thus implying a Z independent mechanism leading to such a behaviour. For states with $n < 40$ our results show that n selective detection is possible, as well as, to a certain extent, a selective detection of states with different angular momenta.

The authors gratefully acknowledge partial financial support from the Sonderforschungsbereich 276 in Freiburg in the early stage of the work. They thank C. Rosen and C. Otto for their technical assistance.

References

1. P. Pillet, H.B. van Linden van den Heuvell, W.W. Smith, R. Kachru, N.H. Tran, T.F. Gallagher, *Phys. Rev. A* **30**, 280 (1984).
2. D. Mariani, W. van de Water, P.M. Koch, T. Bergeman, *Phys. Rev. Lett.* **50**, 1261 (1983).
3. W. van de Water *et al.*, *Phys. Rev. A* **42**, 572 (1990).
4. U. Eichmann, J.L. Dexter, E.Y. Xu, T.F. Gallagher, *Z. Phys. D* **11**, 187 (1989).
5. T.F. Gallagher, in *Atoms in intense laser fields*, Academic Press, edited by M. Gavrilla (Harcourt Brace Jovanovich, New York, 1992), p. 67.
6. T.F. Gallagher, *Rydberg atoms* (Cambridge University Press, Cambridge, 1994).
7. R.R. Freeman, D. Kleppner, *Phys. Rev. A* **14**, 1614 (1976).
8. P.M. Koch, K.A.H. van Leeuwen, *Phys. Rep.* **255**, 289 (1995).
9. P. Pillet *et al.*, *Phys. Rev. Lett.* **50**, 1042 (1983).
10. L.A. Bloomfield, R.C. Stoneman, T.F. Gallagher, *Phys. Rev. Lett.* **57**, 2512 (1986).
11. R.C. Stoneman, D.S. Thomson, T.F. Gallagher, *Phys. Rev. A* **37**, 1527 (1988).
12. R.B. Watkins, W.M. Griffith, M.A. Gatzke, T.F. Gallagher, *Phys. Rev. Lett.* **77**, 2424 (1996).
13. C. Fabre, S. Haroche, P. Goy, *Phys. Rev. A* **18**, 229 (1978).
14. K.A. Smith, F.G. Kellert, R.D. Rundel, F.B. Dunning, R.F. Stebbings, *Phys. Rev. Lett.* **40**, 1362 (1978).
15. L.D. Noordam, H. Stapelfeldt, D.I. Duncan, T.F. Gallagher, *Phys. Rev. Lett.* **68**, 1496 (1992).
16. V. Lange, M.A. Khan, U. Eichmann, W. Sandner, *Z. Phys. D* **18**, 319 (1991).
17. U. Eichmann, V. Lange, W. Sandner, *Phys. Rev. Lett.* **64**, 274 (1990).
18. P. Camus *et al.*, *Phys. Rev. Lett.* **62**, 2365 (1989).
19. R.R. Jones, T.F. Gallagher, *Phys. Rev. A* **42**, 2655 (1990).
20. J. Boulmer, P. Camus, J.-M. Gagne, P. Pillet, *J. Phys. B* **20**, L143 (1987).
21. H.B. van Linden van den Heuvell, T.F. Gallagher, *Phys. Rev. A* **32**, 1495 (1985).
22. C.R. Mahon, J.L. Dexter, P. Pillet, T.F. Gallagher, *Phys. Rev. A* **44**, 1859 (1991).
23. M. Gatzke *et al.*, *Phys. Rev. A* **50**, 2502 (1994).
24. M. Seng, M. Halka, K.-D. Heber, W. Sandner, *Phys. Rev. Lett.* **74**, 3344 (1995).